83 W, 3.1 MHz, square-shaped, 1 ns-pulsed all-fiber-integrated laser for micromachining

Kıvanç Özgören,[1,*] Bülent Öktem,[1] Sinem Yılmaz,[2] F. Ömer Ilday,[2] and Koray Eken[3]

[1] *Institute of Materials Science and Nanotechnology, Bilkent University, 06800 Ankara, Turkey*
[2] *Department of Physics, Bilkent University, 06800 Ankara, Turkey*
[3] *FiberLAST, Ltd., 06531, Ankara, Turkey*

**kozgoren@fen.bilkent.edu.tr*

Abstract: We demonstrate an all-fiber-integrated laser based on off-the-shelf components producing square-shaped, 1 ns-long pulses at 1.03 μm wavelength with 3.1 MHz repetition rate and 83 W of average power. The master-oscillator power-amplifier system is seeded by a fiber oscillator utilizing a nonlinear optical loop mirror and producing incompressible pulses. A simple technique is employed to demonstrate that the pulses indeed have a random chirp. We propose that the long pulse duration should result in more efficient material removal relative to picosecond pulses, while being short enough to minimize heat effects, relative to nanosecond pulses commonly used in micromachining. Micromachining of Ti surfaces using 0.1 ns, 1 ns and 100 ns pulses supports these expectations.

OCIS codes: (140.4050) Mode-locked lasers; (060.2320) Fiber optics amplifiers and oscillators; (140.3390) Laser materials processing.

References and links

1. W. O'Neill and K. Li, "High-quality micromachining of silicon at 1064 nm using a high-brightness MOPA-based 20-W Yb fiber laser," IEEE J. Sel. Top. Quantum Electron. **15**, 462–470 (2009).
2. M. Erdogan, B. Öktem, H. Kalaycioglu, S. Yavas, P. Mukhopadhyay, K. Eken, K. Özgören, Y. Aykac, U. H. Tazebay, and F. Ö. Ilday, "Texturing of titanium (Ti6AI4V) medical implant surfaces with MHz-repetition-rate femtosecond and picosecond Yb-doped fiber lasers," Opt. Express **19**, 10986 (2011).
3. M. Murakami, B. Liu, Z. Hu, Z. Liu, Y. Uehara, and Y. Che, "Burst-mode femtosecond pulsed laser deposition for control of thin film morphology and material ablation," Appl. Phys. Expr. **2**, 042501 (2009).
4. H. A. Haus, "Mode-locking of lasers," IEEE J. Sel. Top. Quantum Electron. **6**, 1173 (2000).
5. V. J. Matsas, T. P. Newson, and M. N. Zervas, "Self-starting passively mode-locked fibre ring laser exploiting nonlinear polarization switching," Opt. Commun. **92**, 61–66 (1992).
6. M. Horowitz, Y. Barad, and Y. Silberberg, "Noiselike pulses with a broadband spectrum generated from an erbium-doped fiber laser," Opt. Lett. **22**, 799–801 (1997).
7. N. J. Doran and D. Wood, "Nonlinear-optical loop mirror," Opt. Lett. **13**, 56 (1988).
8. D. Y. Tang, L. M. Zhao, and L. M. Zhao, "Soliton collapse and bunched noise-like pulse generation in a passively mode-locked fiber ring laser," Opt. Express **13,** 2289–2294 (2005).
9. L. M. Zhao, D. Y. Tang, J. Wu, X. Q. Fu, and S. C. Wen, "Noise-like pulse in a gain-guided soliton fiber laser," Opt. Express **15**, 2145–2150 (2007).
10. L. M. Zhao, D. Y. Tang, T. H. Cheng, and C. Lu, "Nanosecond square pulse generation in fiber lasers with normal dispersion," Opt. Commun. **272**, 431 (2007).
11. P. K. Mukhopadhyay, K. Özgören, I. L. Budunoglu, and F. Ö. Ilday, "All-fiber low-noise high-power femtosecond Yb-fiber amplifier system seeded by an all-normal dispersion fiber oscillator," IEEE J. Sel. Top. Quantum Electron. **15**, 145 (2009).

#150904 - $15.00 USD Received 11 Jul 2011; revised 6 Aug 2011; accepted 9 Aug 2011; published 23 Aug 2011

12. R. P. Scott, C. Langrock, and B. H. Kolner, "High dynamic range laser amplitude and phase noise measurement techniques," IEEE J. Quantum Electron. **7**, 641 (2001).
13. I. L. Budunoğlu, C. Ülgüdür, B. Oktem, and F. Ö. Ilday, "Intensity noise of mode-locked fiber lasers," Opt. Lett. **34**, 2516–2518 (2009).
14. E. J. R. Kelleher, J. C. Travers, E. P. Ippen, Z. Sun, A. C. Ferrari, S. V. Popov, and J. R. Taylor, "Generation and direct measurement of giant chirp in a passively mode-locked laser," Opt. Lett. **34,** 3526–3528 (2009).
15. A. Chong, J. Buckley, W. Renninger, and F. W. Wise, "All-normal-dispersion femtosecond fiber laser," Opt. Express **14**, 10095–10100 (2006).
16. K. Özgören and F. Ö. Ilday, "A filterless all-fiber all-normal dispersion laser," Opt. Lett. **35**, 1296–1298 (2010).
17. H. Hodara, "Statistics of thermal and laser radiation," Proc. IEEE **53**, 696–704 (1965).

1. Introduction

There is much interest in high-power, short-pulsed fiber lasers, which are finding use in various scientific, industrial, and biomedical applications. In particular, the use of short-pulsed fiber lasers in material processing is promising due to their simplicity, low cost and ease of use. For precision micromachining [1], surface texturing [2], pulsed laser deposition [3], and marking, typically relatively low power ($<$ 20 W) pulsed fiber lasers are utilized. The pulse durations and repetition rates range from 100 fs to 100 ns and from 20 kHz to 100 MHz, respectively. High repetition rates and sub-nanosecond pulses are usually generated by mode-locked lasers; low repetition rates and nanosecond pulses rely on Q-switched or directly modulated diode lasers. The region around few MHz is harder to access. Generally, use of mode-locked lasers requires complex pulse picking systems and pulse stretchers and compressors to manage nonlinear effects. The dynamics of mode-locked fiber oscillators are governed by a rich interplay of Kerr nonlinearity, dispersion, and gain [4]. A commonly encountered but usually ignored operation mode is where very long, incompressible pulses are produced. This type of pulses was first observed in Er-doped fiber lasers, which were referred to as noise-like [5, 6]. In cavities utilizing saturable absorbers (SA) with sinusoidal transmission, such as nonlinear polarization evolution or nonlinear loop mirror (NOLM) [7], if the pump power is increased beyond a critical point, the pulse will collapse to a bunch of small pulses [8] due to the peak power clamping effect [9]. The mode characteristically exhibits a broad, smooth spectrum and is evidenced by an autocorrelation trace with a narrow coherence peak on top of a large pedestal [5]. However, if the net cavity dispersion is large and positive, square-shaped, few-nanosecond pulses [10] are formed, which are also incompressible, albeit with a narrower spectrum. Fiber lasers producing such pulses have low repetition rates of around few MHz, which is convenient for reaching microjoule energies through external amplification. In addition, the $\sim$1-ns pulse duration and sub-microsecond pulse spacing is an interesting regime for micromachining, with the expected performance being intermediate to ultrafast pulses and long nanosecond pulses: The longer lasting plasma formation as well as pulse-to-pulse cumulative effects should lead to more efficient ablation. Yet, the pulse duration remains short enough to limit the heat affected zone (HAZ).

In this paper, we demonstrate an integrated Yb-fiber laser producing square-shaped, 1 ns-long pulses at 1.03 μm wavelength with 3.1 MHz repetition rate and 83 W of average power. This is, to the best of our knowledge, the first use of a NOLM [7] in producing square nanosecond pulses. This, in principle, allows the all-fiber-integrated system to be constructed entirely from polarization maintaining (PM) fibers for ultimate environmental stability. We show, using a simple technique, that these pulses indeed have an incompressible chirp. Finally, we make a comparison of the Ti-surface micromachining performance using 0.1 ns, 1 ns and 100 ns pulses.

2. Experimental results and discussion

Schematic of the experimental setup can be seen in Fig. 1. The oscillator comprises of a 0.7-m-long Yb-doped fiber, followed by a 30% output coupler, a 10-nm bandpass filter, an inline

#150904 - $15.00 USD Received 11 Jul 2011; revised 6 Aug 2011; accepted 9 Aug 2011; published 23 Aug 2011

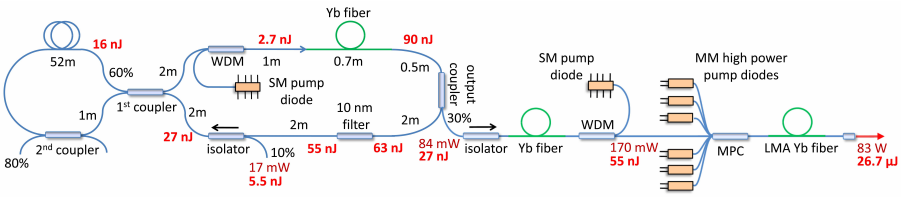

Fig. 1. Schematic of the oscillator-amplifier setup. WDM: Wavelength-division multiplexer; LMA: Large mode area; MPC: Multi pump combiner. The fiber lengths, powers and pulse energies are indicated.

isolator to ensure unidirectional operation and a 50-m-long Sagnac loop. The fundamental repetition rate of the cavity is 3.1 MHz. Although the oscillator can operate without the bandpass filter, its presence sets the central wavelength and improves stability. As pump source, we use a fiber-coupled single-mode 980-nm diode laser delivering a maximum power of 650 mW. The oscillator output seeds a two-stage all-fiber amplifier, similar to the system described in Ref. [11]. A core-pumped preamplifier stage is used to increase the signal level up to 170 mW. The power amplifier stage is composed of a multiple-port pump-signal combiner (MPC) and six pump diodes coupled to 105 μm-core multimode (MM) fibers, each delivering up to 25 W. The double-clad Yb-doped fiber of the power amplifier in this study has 25 μm core diameter, core numerical aperture of 0.07 and cladding diameter of 250 μm.

Pulsed operation of the oscillator is attained readily. The nonlinear phase shift accumulated in the CW and CCW directions in the loop can be calculated by using $\Delta\phi = \frac{2\pi}{\lambda} n_2 \frac{P}{A_{\text{eff}}} L$, where n_2 is the Kerr nonlinearity coefficient, P is the peak power and L is the effective propagation distance. Using experimental values, the relative phase shift between two counter propagating beams is estimated to be close to $\sim \pi$. Thus, the laser converges on a state supporting a nearly square-shaped pulse, which is maximally transmitted through the NOLM. This is to be expected, given that the extra long pulse duration and random chirp nullifies the influence of dispersion. The pulse duration is determined by the intra-cavity energy with the peak power remaining constant. This is verified by changing the pump power from 350 mW to 650 mW. As expected, the pulse duration increases linearly with output power; no change in spectral width or shape is observed (Fig. 2(a)). Figure 2(b) shows the optical spectrum recorded from the 10% monitor port of the isolator. The temporal profile of the pulses are measured with a 50-GHz sampling oscilloscope and 12-GHz photodiode, with a combined rise time of $\sim$30 ps (Fig. 2(c)). The inset shows the RF spectrum of a comb line, which is clean of sidebands and modulations down to -70 dB, indicating low-noise operation and absence of Q-switching instability. The timing jitter inferred from a single-sideband phase noise measurement of the laser is calculated to be 1.15 ps over the frequency range 1 kHz to 1.55 MHz. Although this value should be taken as an upper limit due to insufficient suppression of adjacent comb lines (the low repetition rate makes it difficult to select a single comb line), it is far larger than the expected value for a properly mode-locked laser. The short-term power stability of the pulse train is further characterized by its relative intensity noise (RIN) spectrum measured using the standard method [12, 13]. The intensity noise, integrated over the range of 3 Hz to 250 kHz, is measured to be 0.66% for the oscillator and 1.86% after the power amplifier. Increase in the intensity noise after the power amplifier is attributed to pump fluctuations coupled from the relatively noisy MM pump diodes [11]. At full pump power, the amplifier output reaches 83 W of average power, corresponding to $\sim$ 25 μJ of pulse energy and 25 kW of peak power. Figure 2(d) shows the optical spectrum of power amplifier at various output powers. The growing influence of Raman amplification is evident, confirming the high peak power of the source. The formation of a Raman-induced red-shifted

#150904 - $15.00 USD Received 11 Jul 2011; revised 6 Aug 2011; accepted 9 Aug 2011; published 23 Aug 2011

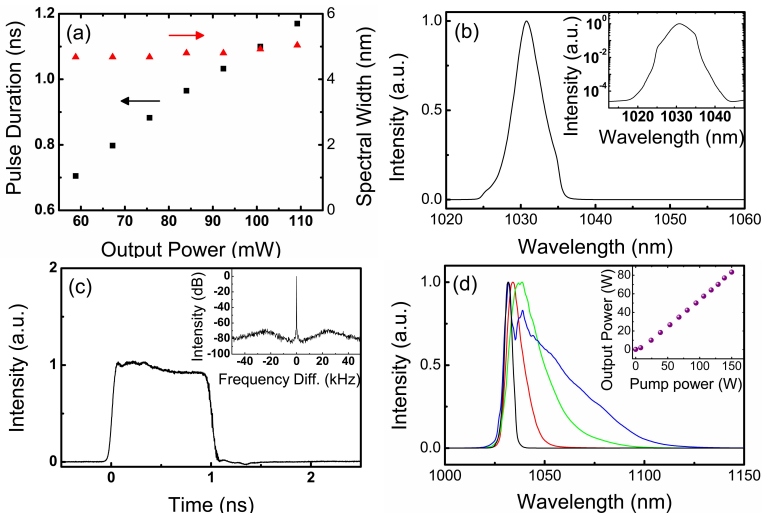

Fig. 2. (a) Variation of pulse duration (black) and spectral width (red) with the output power of the oscillator. (b) Optical spectrum of the pulse train measured at the 10% output port. Inset: Optical spectrum in logarithmic scale. (c) Pulse shape measured with a 30 ps-rise time sampling scope. Inset: RF spectrum of an individual comb line demonstrating low-noise operation. (d) Optical spectra measured directly from the oscillator (black), and from the amplifier output at powers of 26.6 W (red), 57.4 W (green), 83 W (blue). Inset: output power vs. pump power.

peak is not detrimental to applications that depend solely on peak power since the Raman part of the spectrum is temporally overlapping the main pulse. Nevertheless, the pulse duration is confirmed to be unchanged at all power levels.

It is reasonable to ask if the oscillator simply has a giant, potentially very complex, but well-defined chirp, varying monotonically across the pulse. Although square-like pulsed operation has been extensively studied, no direct confirmation of their phase or chirp profiles has been reported. We use a simple setup to measure the chirp on the pulses (Fig. 3(a)), similar to the spectrogram measurements in [14]. The oscillator's output is sent to a Mach-Zehnder interferometer, where a tunable bandpass filter is placed in one arm. The filtering action is obtained with a diffraction grating followed by a fiber collimator, which functions as a Gaussian aperture. The tuning of the central wavelength and the bandwidth of the filter is achieved by rotating the grating and by adjusting the distance to the fiber collimator, respectively. The output of the interferometer is sent to an optical spectrum analyzer along with a fast photodiode connected to the sampling scope. If the pulse has a well-defined and monotonic, albeit nonlinear temporal chirp, the spectral components constituting the pulse should be spread in time and also have a certain degree of temporal localization. Thus, spectrally filtering the pulse should produce shorter temporal waveforms, and the arrival time of different portions of the spectrum to the sampling scope should differ. We use a properly mode-locked all-normal dispersion (ANDi) laser [15] as reference for this measurement. The cavity setup is similar to that of Ref. [16] and its output is chirped to a duration of $\sim$ 100 ps. While spectral filtering of the chirped pulses for the reference laser leads to shorter pulses, the pulse duration for the square-pulsed laser is unchanged (Figs. 3(b) and 3(c)). A spectrogram is obtained by recording the pulse width and temporal position against central wavelength for the filtered pulses. While results for the reference laser confirms the expected linear chirp (Fig. 3(e)), for the 1 ns laser, the spectral components have virtually no fixed localization within the temporal envelope of the unfiltered

#150904 - $15.00 USD Received 11 Jul 2011; revised 6 Aug 2011; accepted 9 Aug 2011; published 23 Aug 2011

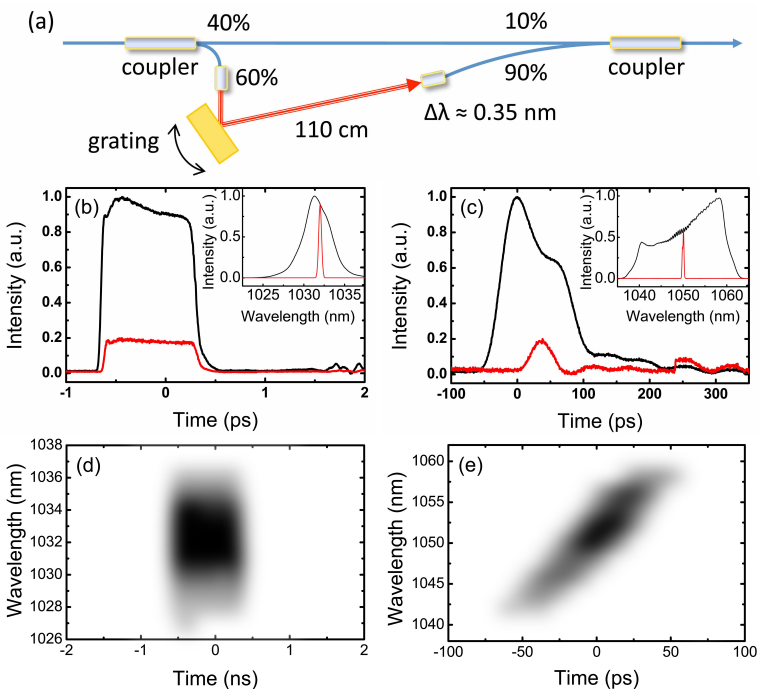

Fig. 3. (a) Experimental setup for the pulse chirp measurement. For (b) NOLM and (c) reference lasers, temporal and spectral (insets) profiles of the spectrally filtered (red) and unfiltered pulses (black). Spectrograms of (d) NOLM and (e) reference lasers are shown where gray-scaling indicates intensity. The data has been smoothened using Gaussian averaging to reduce graininess.

pulse (Fig. 3(d)). These results demonstrate conclusively that the square-like pulses are incompressible. The phase noise and RIN after the tunable filter are measured as 2.16 ps and 5.67%, respectively. The spectral filtering reduces the optical bandwidth by about 10 times. The small variation of the phase noise and the 10-fold increase of the RIN are consistent with the modes of the cavity having randomly fluctuating phases, similar to the bandwidth-scaling of intensity noise due to statistical fluctuations of the electromagnetic modes for an amplified spontaneous emission source [17].

3. Micromachining of Ti surfaces

In order to assess the utility of the system in material processing, we micromachine depressions on a polished titanium surface. The spot size is 20 μmm. Three seed sources are in these experiments, connected to the same amplifier and followed by exactly the same delivery and focusing optics: the nanosecond system described here (1 ns pulses at 3.1 MHz), a commercial fiber laser set to produce 100 ns pulses at 31 kHz and a properly modelocked ANDi fiber laser with 115 ps pulses at 27 MHz. All three systems are adjusted to yield the same peak power for the same average power. Figure 4 shows the SEM images of holes produced at 3 W and 0.5 s exposure time in comparison. The depth of the holes is increasing with the pulse duration, indicating increased efficiency of material removal. On the other hand, the heat affected zone (HAZ) is significantly larger for the 100 ns pulses compared with the 0.1 ns and 1 ns pulses and the uniformity is poorer. A clear indication of the similarity of the 0.1 ns or 1 ns results and their distinction from the 100 ns results is the formation of similar sub-micron-sized crystalline

#150904 - $15.00 USD Received 11 Jul 2011; revised 6 Aug 2011; accepted 9 Aug 2011; published 23 Aug 2011

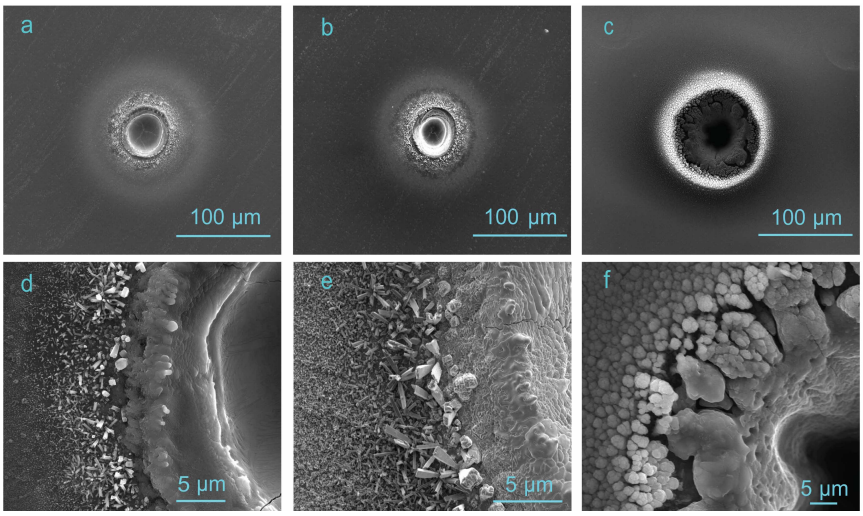

Fig. 4. Wells on the polished Ti surface drilled by (a) 115 ps, (b) 1 ns and (c) 100 ns pulses in comparison. (d,e,f) show corresponding close-up scanning electron microscope (SEM) images.

structures, which are completely absent from the 100 ns results. Much of the formed structure is TiO_2. Energy-dispersive X-ray spectrocopy measurements were performed, which indicate that the oxidation level is significantly larger for the 100 ns pulses. This can be explained by higher temperatures reached when using long pulses. These results are consistent with our qualitative expectations on the performance of 1 ns-long pulses.

4. Conclusion

In conclusion, we have demonstrated the generation of 1-ns-long pulses from an all-fiber-integrated Yb laser cavity, which uses a NOLM to initiate low-repetition-rate (3.1 MHz) pulsed operation, eliminating the need for pulse picking. We demonstrate, to our knowledge, the first use of such pulses in micromachining. Since beam propagation is fiber-guided everywhere, the laser system is extremely robust. We also verified using a simple setup that these pulses indeed lack a well-defined chirp and are, therefore, incompressible. Nevertheless, the intensity fluctuations of the oscillator are found to be low ($< 0.7\%$). We compared the micromachining performance of the 1 ns, 3.1 MHz laser system with an industrial fiber laser producing 100 ns-long pulses at 31 kHz and an ultrafast fiber laser system producing 115 ps-long pulses at 27 MHz, while maintaining the same average and peak power. The results indicate that the repeatability and uniformity of the micromachined surfaces are similar for the 1 ns and 0.1 ns lasers and significantly better than those of the 100 ns laser. The amount of ablated material is higher for the 1 ns laser than for the 0.1 ns, but lower than the 100 ns laser. This regime occupies a large portion of the phase space for long cavity lasers, exhibiting a high tolerance to environmental perturbations. In addition, the all-fiber-integrated architecture improves stability and allows for direct beam delivery to the sample via fiber.

Acknowledgments

This work was supported by the SANTEZ Project No. 00255.STZ.2008-1.

#150904 - $15.00 USD Received 11 Jul 2011; revised 6 Aug 2011; accepted 9 Aug 2011; published 23 Aug 2011